Closed-Loop Control of Functional Neuromuscular Stimulation

NIH Neuroprosthesis Program Contract Number N01-NS-6-2338
Quarterly Progress Report #15
October 1, 1999 to December 31, 1999

Investigators:
Patrick E. Crago, Ph.D.
Clayton L. Van Doren, Ph.D.
Warren M. Grill, Ph.D.
Michael W. Keith, M.D.
Kevin L. Kilgore, Ph.D.
Joseph M. Mansour, Ph.D.
Wendy M. Murray, PhD.
P. Hunter Peckham, Ph.D.
David L. Wilson, Ph.D.

Cleveland FES Center

Departments of Biomedical Engineering,
Mechanical and Aerospace Engineering,
and Orthopaedics
Case Western Reserve University
and MetroHealth Medical Center

1. SYNTHESIS OF UPPER EXTREMITY FUNCTION

The overall goals of this project are to (1) measure the biomechanical properties of the neuroprosthesis user's upper extremity and incorporate those measurements into a complete model with robust predictive capability, and (2) use the predictions of the model to improve the grasp output of the hand neuroprosthesis for individual users.

1. a. BIOMECHANICAL MODELING: PARAMETERIZATION AND VALIDATION

Purpose

In this section of the contract, we will develop methods for obtaining biomechanical data from individual persons. Individualized data will form the basis for model-assisted implementation of upper extremity FNS. Using individualized biomechanical models, specific treatment procedures will be evaluated for individuals. The person-specific parameters of interest are tendon moment arms and lines of action, passive moments, and maximum active joint moments. Passive moments will be decomposed into components arising from stiffness inherent to a joint and from passive stretching of muscle-tendon units that cross one or more joints.

Progress Report

1. a. i. MOMENT ARMS VIA MAGNETIC RESONANCE IMAGING

Abstract

No activity took place with regard to this project this quarter.

1.a.ii. PASSIVE AND ACTIVE MOMENTS

Abstract

Previously, we reported making modifications to our recording setup to obtain additional information regarding parameters which affect the passive properties of the MP joint of the finger. During this quarter, we investigated further parameters which affect the passive properties of the finger MP joint, including the position and/or restraint of the other fingers, forearm pronation/supination and elbow flexion.

Purpose

The purpose of this project is to characterize the passive properties of normal and paralyzed hands. This information will be used to determine methods of improving hand grasp and hand posture in FES systems.

Progress Report

During this quarter we first investigated the effect of the position and/or restraint of the long, ring and small fingers when the MP moment of the index finger was measured. In previous studies, the other fingers were constrained at approximately 20º flexion in order to avoid interference with the splint and torque measurement equipment. In order to determine the impact of constraining the fingers, we first designed a newer splint, with lower profile and less potential interference with the other fingers. Passive moments of the index MP joint, at various wrist angles were recorded with the other fingers free to move, or constrained at either 30º extension, 20º flexion or 80º flexion.

The graphs in Figure 1.a.ii.1. show the effects of constraining the fingers for three different wrist angles. The curves shown are the moment vs angle curves (MAC) for each of the finger constraints at a specific wrist angle. The top graph shows the MACs with the wrist extended, the middle graph with wrist in neutral and the bottom graph with wrist flexed. The curves demonstrate a need to allow the other fingers to move freely in order to achieve the best representation of the passive moments due to structures other than the skin. The graphs also show that if the fingers must be constrained, setting the fingers at 20º flexion has the least effect on the characteristics of the MAC.

Another area we examined this quarter was the effect of elbow angle on the passive properties of the fingers. Since the Flexor Digitorum Superficialis and Extensor Digitorum Communis originate proximal to the elbow, we anticipated that changes in the elbow angle would affect the passive properties of the MP joint by changing the length of these tendons the results indicate tat there is a measureable effect of elbow angle on the MP MACs. Figure 1.a.ii.2 shows the MP moment angle curves at various elbow with the wrist extended to 60º. It can be seen from the curves that the elbow angle must be considered when looking at data in which the finger flexors contribute significantly to the measured moments.

Based upon this observation, a further modification was made to the measurement setup to include the measurement of elbow flexion and forearm pronation/supination. This was accomplished using a three axis accelerometer strapped to the upper arm. Additional modifications were required to the data collection software to include the appropriate transformations from the accelerometer measurements to elbow flexion and forearm pronation.

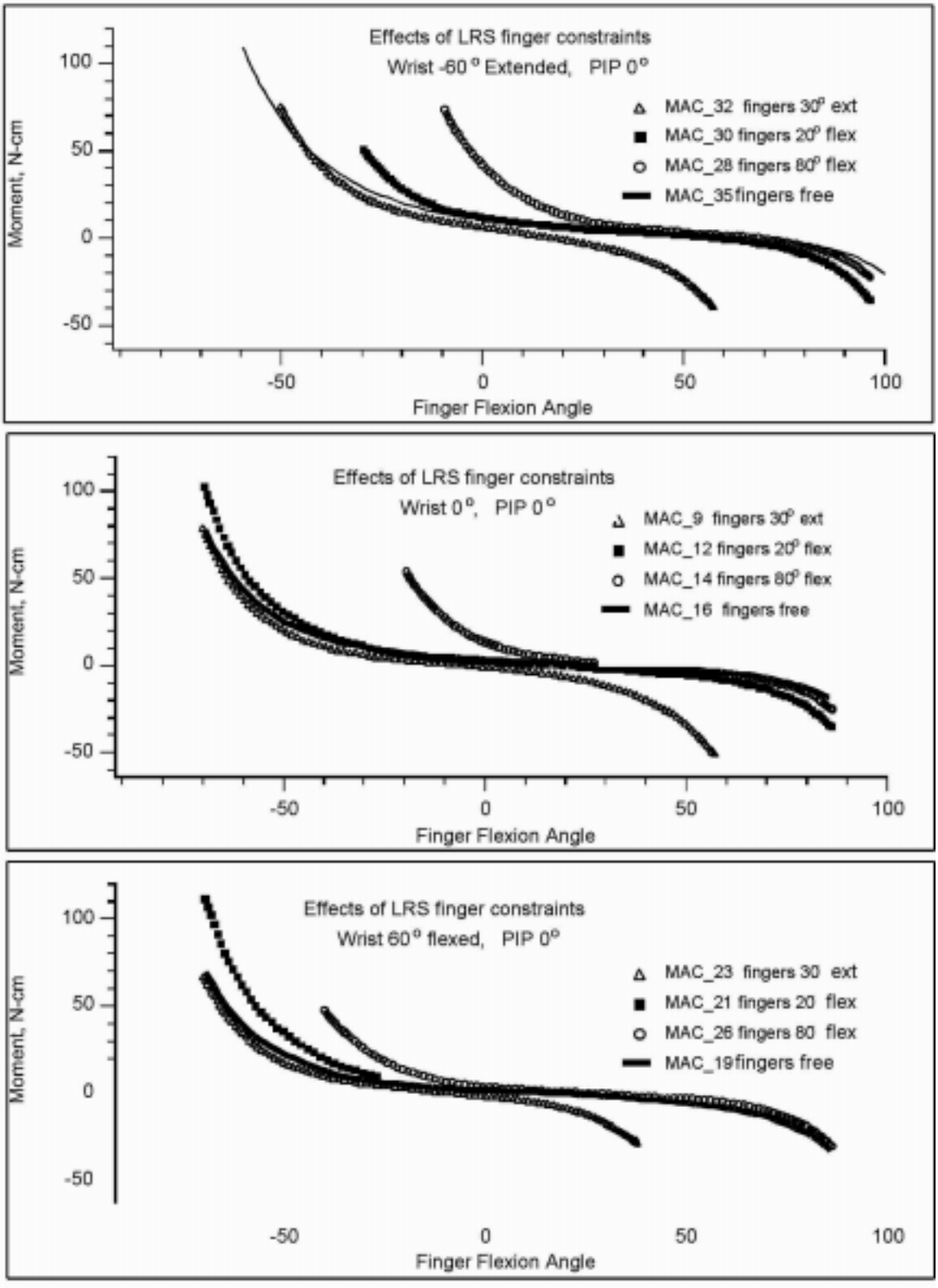

Figure 1.a.ii. 1. Moment Angle Curves of the index finger MP joint for three wrist angles and various constraints of long, ring and small fingers.

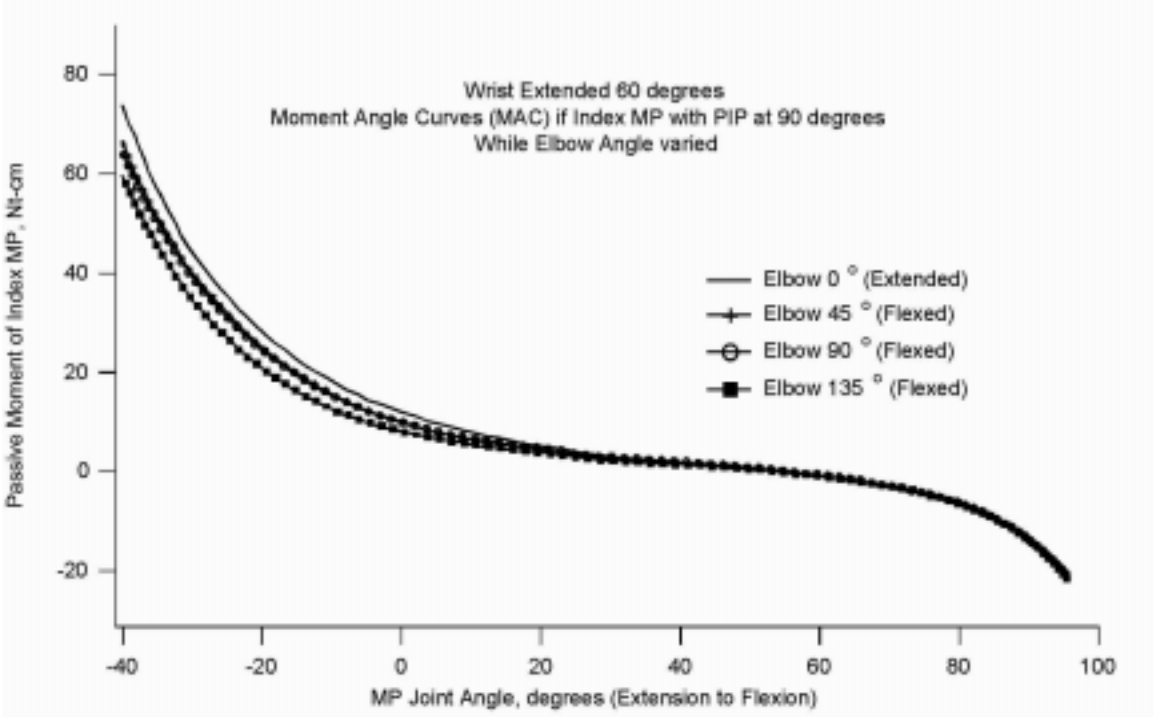

Figure 1.a.ii. 2. Moment Angle Curves of the MP joint of the index finger, with wrist at 60º extension and elbow at various flexion angles.

Plans for Next Quarter

Next quarter we plan to construct a physical model of the index finger which includes intrinsic and extrinsic muscles and use it to test and verify our mathematical model for separating intrinsic and extrinsic components of the passive properties. We also intend to collect further data which will include the elbow flexion and forearm pronation angle, in order to include these in our mathematical model.

1. b. BIOMECHANICAL MODELING: ANALYSIS AND IMPROVEMENT OF GRASP OUTPUT

Abstract

Our biomechanical model of the Br-ECRB tendon transfer and preliminary clinical assessments of wrist function indicate that the ability to voluntarily extend the wrist depends on the position of the elbow after the tendon transfer. We measured the active range of motion at the wrist, passive range of motion at the wrist, lateral pinch strength, voluntary wrist extension strength, and voluntary elbow extension strength of one individual with the Br-ECRB tendon transfer. The wrist extension position that could be maintained against gravity and lateral pinch strength decreased with elbow flexion in this subject. In addition, when the wrist was extended 30˚, the isometric wrist extension moment generated during maximum voluntary contraction decreased when the elbow was flexed 120˚ compared to when it was fully extended. The isometric elbow extension moment generated during maximum voluntary

contraction was at least 2.5 times greater than the elbow flexion moment generated during wrist extension. These data support the biomechanical model, which suggests that changes in the force-generating capacity of the brachioradialis that occur as a function of elbow position limit wrist function after the Br-ECRB tendon transfer.

Purpose

The purpose of this project is to use the biomechanical model and the parameters measured for individual neuroprosthesis users to analyze and refine their neuroprosthetic grasp patterns.

In the past quarter, we have evaluated how the passive moment-generating capacity of the tight and slack Br-ECRB transfer (described in previous progress reports) influences gravity-assisted wrist flexion. The net passive moment at the wrist joint (before a Br-ECRB transfer) was compared to the passive wrist extension moment generated by the transfer to estimate the range of wrist postures where gravity-assisted wrist flexion is possible.

Progress Report

In the past quarter, we have continued to evaluate wrist function after the Br-ECRB tendon transfer. Active range of motion against gravity, passive range of motion, and lateral pinch strength were measured in different elbow positions in an individual with a Br-ECRB tendon transfer. In addition, we performed quantitative measurements of the wrist extension moment generated during maximum voluntary contraction, the elbow extension moment generated during maximum voluntary contraction, and the elbow flexion moment generated during wrist extension as a function of elbow position in the same individual.

Clinical assessments of wrist function in an individual with a Br-ECRB tendon transfer

In previous progress reports, we have described clinical assessments of wrist function in a number of individuals with the Br-ECRB tendon transfers. We believe that clinical measurements and quantitative assessments of voluntary strength and passive joint properties made in the same subjects will help us to assess the sources of deficits in post-operative wrist function.

The maximum position of wrist extension this subject could maintain against gravity decreased as the elbow was flexed (Fig. 1.b.1). Relative to full elbow extension, the maximum position decreased by 2˚ when the elbow was flexed 90˚ and decreased by 27˚ when the elbow was flexed 120˚. The rest position of the wrist against gravity was in wrist flexion. When the elbow was flexed 120˚, the rest position increased by 23˚ flexion compared to when the elbow was extended. At 90˚ elbow flexion, an increase of 11˚ wrist flexion was observed. Also, the passive range of motion in wrist flexion increased by 9˚ when the elbow was flexed 90˚, and increased by 16˚ when the elbow was flexed 120˚. The passive range of motion in wrist extension did not vary with elbow position. Lateral pinch strength decreased with elbow flexion.

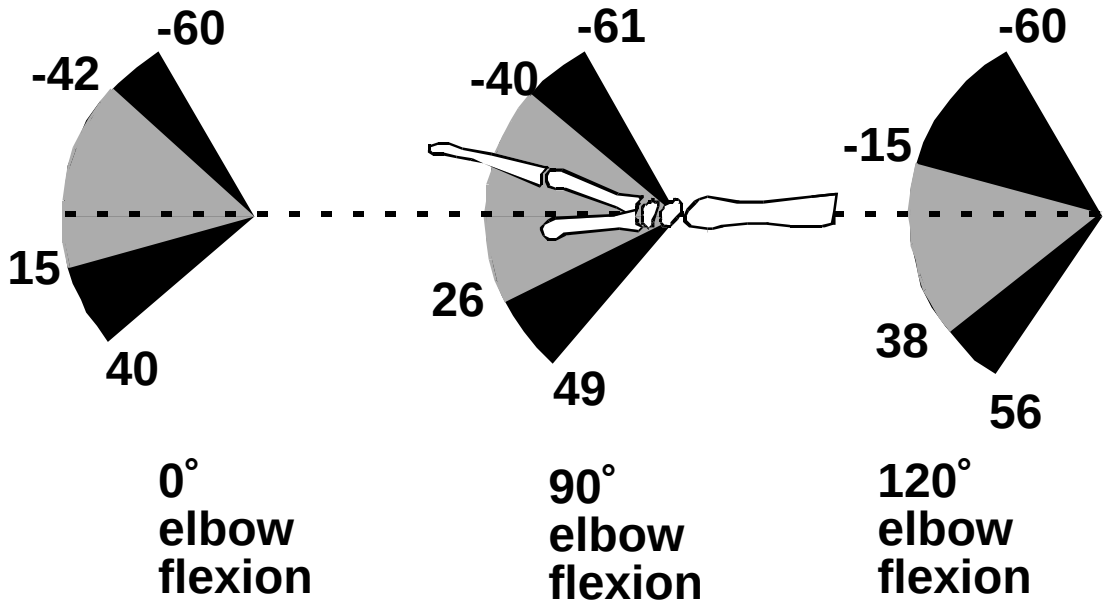

Fig. 1.b.1. Passive range of motion in wrist extension and wrist flexion (indicated by shaded black region) and active range of motion in wrist extension against gravity (indicated by shaded gray region) measured in one subject in three elbow postures. Negative numbers indicate wrist extension, positive numbers indicate wrist flexion. The maximum position of wrist extension decreased as the elbow was flexed. The rest position of the wrist against gravity became more flexed as the elbow was flexed. Also, the passive range of motion in wrist flexion increased as the elbow was flexed.

Quantitative measurements of strength at the wrist in an individual with a Br-ECRB tendon transfer

We measured the isometric wrist extension moment generated during maximum voluntary contraction in this subject using the wrist moment transducer (WMT, described in previous progress reports). Informed consent was obtained prior to the measurement protocol. The device was mounted across the wrist by securing it to two casts made for the subject's hand and forearm. The cast of the hand extended from the base of the thumb to the proximal interphalangeal joints. The cast of the forearm extended from approximately five centimeters distal to the elbow joint to the proximal aspect of the radial styloid process. The casts allowed movement in both wrist flexion/extension and radial/ulnar deviation. The subject was seated in his wheelchair. His shoulder was positioned in 90˚ abduction, 0˚ internal/external rotation, 0˚ horizontal flexion, and his forearm was positioned in 0˚ pronation/supination. Gravity opposes wrist extension in this arm posture. The subject's upper arm and forearm rested on a table, while his wrist and hand extended beyond the edge of the table.

Measurements of the isometric wrist extension moment generated during maximum voluntary effort were obtained on two separate days. On the first day, three measurements were obtained in all combinations of three wrist postures (30˚ flexion, 0˚ flexion/extension or neutral, and 30˚ extension) and four elbow positions (0˚ elbow flexion or full extension, 30˚ elbow flexion, 90˚ elbow flexion, and 120˚ elbow flexion). On the second day, two or four trials were performed at each combination of two wrist

positions (neutral and 30˚ extension) and two elbow positions (full extension and 120˚ elbow flexion). The wrist and wrist moment transducer were positioned and secured in the desired position, and wrist extension moment was measured at each of the different elbow postures before the wrist was re-positioned and the measurements at different elbow flexion angles were repeated. Data collection was first initiated, then the subject was instructed to provide a maximum wrist extension moment over a period of 4 seconds. The subject received visual feedback of the wrist extension moment displayed on an oscilloscope, which also displayed a target larger than he could actually produce to encourage maximal effort. The wrist moment transducer senses both flexion/extension and radial/ulnar deviation moments. The moments during each trial were sampled (after anti-aliasing filtering) by a National Instruments AT-MIO-64E-3 board at 300 Hz for 12 seconds. An electrogoniometer (Penny and Giles, United Kingdom) was mounted on the cast and the output from the electrogoniometer was also sampled to monitor any changes in wrist position that might have occurred during each trial.

After data collection was completed, the maximum wrist extension moment was calculated offline using a MATLAB analysis program. Each channel of data was converted from the voltage output of the transducer to a moment given the calibration equations of the device. We calculated a baseline for each channel, the average moment over the first two seconds of data collection (when the subject was at rest), and subtracted this baseline from the data. Each channel was then digitally filtered using a Butterworth filter to reduce the noise in the signal and the maximum moment that was maintained for at least 0.5 seconds was identified. The maximum wrist extension moment and the corresponding deviation moment were calculated for each trial as the averages of the moments generated over this time period. On each day, the maximum wrist extension moment for each set of elbow and wrist configurations was taken as the maximum of the multiple trials performed for that configuration on that day. The change in wrist position during maximum voluntary contraction was calculated by subtracting the average electrogoniometer output during the identified time period from the electrogoniometer baseline.

The isometric wrist extension moment generated during maximum voluntary contraction decreased with elbow flexion when the wrist was extended and increased with elbow flexion when the wrist was in the neutral position or was flexed. When the wrist was extended 30˚, the isometric wrist extension moment was greatest when the elbow was fully extended (45.9 Ncm) and least when the elbow was flexed 90˚ (27.7 Ncm, Fig. 1.b.2). When the wrist was in either the neutral position or flexed 30˚, the isometric moment was greatest in the position where the elbow was flexed 120˚ (48.6 Ncm and 44.3 Ncm, respectively). When the wrist was in the neutral position, the isometric moment was least when the elbow was flexed 30˚ (37.3 Ncm). When the wrist was flexed 30˚, the isometric moment was least when the elbow was fully extended (27.8 Ncm). The data described here are the maximums from the first day of measurements.

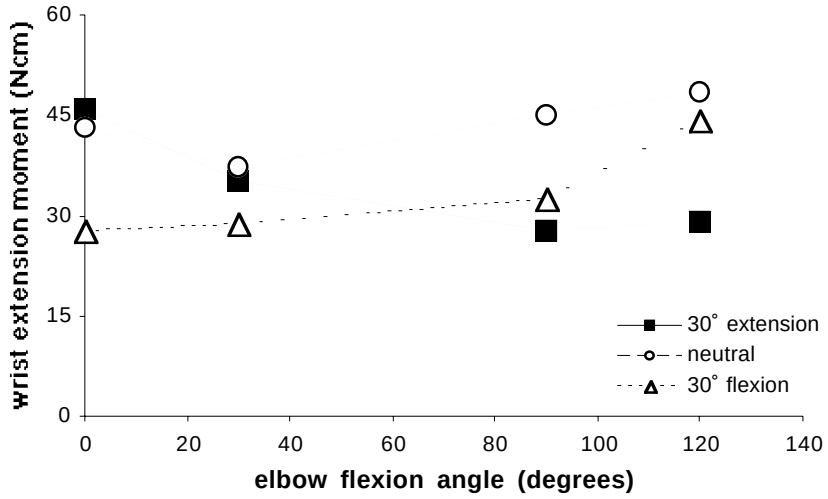

Fig. 1.b.2. Isometric wrist extension moment produced during maximum voluntary contraction as a function of elbow flexion angle, measured on day 1. When the wrist was extended 30˚ (filled squares), voluntary wrist extension strength decreased as the elbow was flexed. When the wrist was neutral (0˚ flexion/extension, open circles) or flexed 30˚ (open triangles), voluntary wrist extension strength increased as the elbow was flexed.

The data set from the second day of measurements showed the major conclusions from the measurements from the first day were repeatable. That is, for this subject, the isometric wrist extension moment generated during maximum voluntary contraction decreases with elbow flexion when the wrist is extended 30˚ and increases with elbow flexion when the wrist is in neutral (Fig. 1.b.3). On the second day of testing, we reduced the number of elbow positions where wrist extension strength was measured from four to two (0˚ elbow flexion and 120˚ elbow flexion), and the number of wrist positions from three to two (30˚ extension and the neutral wrist postion). The order in which the wrist and elbow positions were tested was also altered. These changes in the protocol were implemented to ensure the previously observed differences were not a result of muscle fatigue.

Quantitative measurements of strength at the elbow in an individual with a Br-ECRB tendon transfer

Because the brachioradialis is an elbow flexor, activating the Br-ECRB tendon transfer to generate wrist extension also produces an elbow flexion moment. Because of this, candidates for the Br-ECRB tendon transfer must have elbow extension strength adequate to stabilize the elbow joint during wrist extension. Because individuals with C5 level tetraplegia have paralyzed elbow extensors, the posterior deltoid to triceps (PD-TRI) tendon transfer is used to provide active elbow extension. To test the elbow extension strength provided by the PD-TRI transfer, we measured the isometric elbow extension moment during maximum voluntary contraction and compared it to the elbow flexion moment generated during wrist extension in this subject. Elbow flexion and extension moments were measured using the elbow moment transducer (EMT, described in previous progress reports).

The protocol for measurement of elbow extension and flexion moments was similar to that described for measurement of wrist extension strength. The subject was seated in his wheelchair. His shoulder and forearm were positioned as described for the WMT measurements, so that gravity opposed wrist extension. The EMT was secured to a large pole that allows the position and orientation of the device to be easily altered relative to the subject. The pole also provides support for the subject's arm, preventing fatigue of the shoulder muscles. The EMT was mounted on his upper arm and forearm using Bledsoe braces.

Measurements of the maximum isometric elbow extension moment and the elbow flexion moment generated during wrist extension were obtained in three elbow positions (30˚ elbow flexion, 90˚ elbow flexion, and 120˚ elbow flexion). Three measurements of maximum elbow extension moment were obtained in each elbow position, followed by one measurement of the elbow flexion moment generated during wrist extension. The protocol for data collection and analysis is the same as described for the measurements with the WMT.

The data indicates that this subject is capable of balancing the elbow flexion moment generated by the Br-ECRB tendon transfer during wrist extension using his PD-TRI transfer. The isometric elbow extension moment generated by the PD-TRI transfer during maximum voluntary contraction was at least 2.5 times greater than the isometric elbow flexion moment generated during wrist extension in all three of the elbow positions tested (Fig. 1.b.4). The maximum elbow extension moments ranged from 260 Ncm at 90˚ elbow flexion to 200 Ncm at 30˚ elbow flexion. The elbow flexion moments ranged from 80 Ncm at 90˚ and 30˚ elbow flexion, to 86 Ncm at 120˚ elbow flexion. We conclude that the decrease in the maximum position of wrist extension that could be maintained against gravity at 120˚ elbow flexion is not due to insufficient elbow extension strength in flexed elbow postures in this subject.

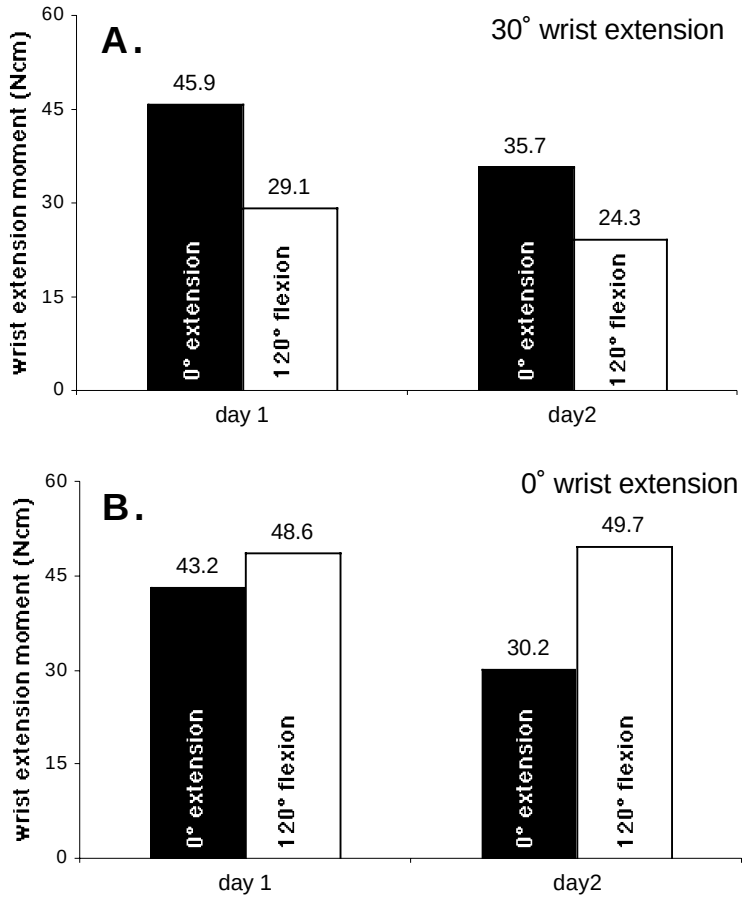

Fig. 1.b.3. (A). Maximum isometric wrist extension moment measured when the wrist was extended 30˚ in two elbow postures (full extension (0˚) and 120˚ elbow flexion) on two different days. (B). Maximum isometric wrist extension moment measured when the wrist was in the neutral position (0˚ flexion/extension) in two different elbow postures on two different days. The data illustrate that wrist extension strength decreases with elbow flexion when the wrist is extended but that wrist extension strength increases with elbow flexion when the wrist is in neutral.

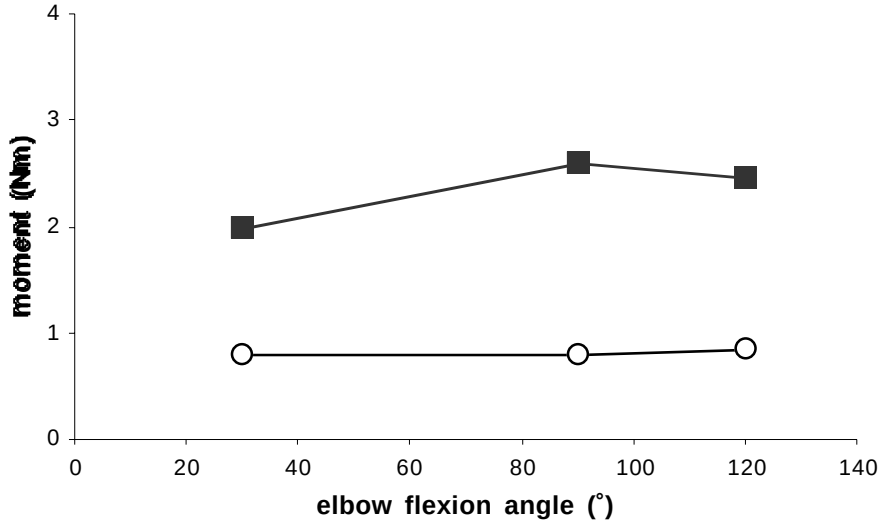

Fig. 1.b.4. Magnitude of the elbow extension moment generated during maximum voluntary contraction (filled squares) and elbow flexion moment generated during wrist extension (open circles) in different elbow postures. Voluntary elbow extension strength was greater than the elbow flexion moment generated during wrist extension.

Summary

The clinical assessments of wrist function and quantitative measurements of wrist and elbow extension strength illustrate that wrist extension depends on elbow position in this subject. These data support the biomechanical model, which suggests that changes in the force-generating capacity of the brachioradialis that occur as a function of elbow position limit wrist function after the Br-ECRB tendon transfer.

Plans for Next Quarter

In the next quarter we plan to continue quantifying wrist function and strength in individuals with the Br-ECRB tendon transfer. We also plan to develop the experimental protocol for measuring passive wrist joint properties in these subjects. In addition, we plan to submit a paper for publication that summarizes the biomechanical model simulations of wrist function after the Br-ECRB tendon transfer.

2. CONTROL OF UPPER EXTREMITY FUNCTION

Our goal in the five projects in this section is to either assess the utility of or test the feasibility of enhancements to the control strategies and algorithms used presently in the CWRU hand neuroprosthesis. Specifically, we will: (1) determine whether a portable system providing sensory feedback and closed-loop control, albeit with awkward sensors, is viable and beneficial outside of the laboratory, (2) determine whether sensory feedback of grasp force or finger span benefits performance in the presence of natural visual cues, (of particular interest will be the ability of subjects to control their grasp output in the presence of trial-to-trial variations normally associated with grasping objects, and in

the presence of longer-term variations such as fatigue), (3) demonstrate the viability and utility of improved command-control algorithms designed to take advantage of forthcoming availability of afferent, cortical or electromyographic signals, (4) demonstrate the feasibility of bimanual neuroprostheses, and (5) integrate the control of wrist position with hand grasp.

2. a. HOME EVALUATION OF CLOSED-LOOP CONTROL AND SENSORY FEEDBACK

Abstract

In this quarter we continued bench tests of the feedback system prototype after additional field tests suggested re-investigation of deficiencies in the basic i/o characteristic cited in the previous report. The results suggest several straightforward changes to the design, including adding a changeable resistor in parallel with the FSR.

Purpose

The purpose of this project is to deploy a portable hand grasp neuroprosthesis capable of providing closed-loop control and sensory feedback outside of the laboratory. Our goal is to evaluate whether the additional functions provided by this system benefit hand grasp outside of the laboratory.

Progress Report

In this quarter, we continued bench-top evaluations of the prototype, single-channel, grasp-force feedback system. These evaluations were necessary to correct the performance deficiencies noted in the previous report. First, we re-calibrated the FSR and found that its resistance-force characteristic was not described by a power function as well as previously observed. The measurements were made as before using the apparatus shown in Fig. 2.a.1, Progress Report 14. The force sensor was placed in series with a spring-loaded manipulandum containing a commercial load cell (Entran ELF-1000), and compressed in a vise. Forces were measured with the commercial load cell, while the resistance was measured with a DMM. Whether the change in performance is due to aging of the sensor or to choice of a different particular FSR is not known, but either case motivates a re-design to minimize the effects of such variations. We propose the simple addition of a parallel resistor to both improve the sensor characteristic and to permit adjustments for changes in sensor performance. Fig. 2.a.1 shows the resistance of a particular FSR sensor (including the foam layer and rigid overlay) as a function of force, as well as the best-fit power function. The latter fails to follow the actual curvature of the characteristic at low forces. The latter is likely responsible for the curvature observed in the net force-current characteristic of the stimulator reported previously. The figure also shows that adding a resistor in parallel with the FSR reduces both slope (exponent) and the curvature of the characteristic, improving the power-function approximation. Moreover, making such a resistor replaceable would allow re-adjustment of the sensor

characteristic as a given sensor ages or if a sensor is replaced. We propose adding the parallel resistor in the next iteration of the stimulator.

We note that the reduction of the FSR exponent also necessitates a minor design change in the configuration of the analog computational unit (AD 538). The device is currently configured to produce an i/o power function with an exponent less than unity, but larger exponents will be required given the FSR modification. Fig. 2.a.2 shows simulated

Force-to-current transfer functions calculated using (a) the FSR response with a 5K parallel resistance, (b) the AD 538 configured for exponents >1. Note that the responses are much closer to the desired nominal power function relationships (compare to Fig. 2.a.2 of the previous report). The figure also shows that the exponent adjustment should accommodate a wide range of values depending on the dynamic range of a particular subject.

We will also take the opportunity to add jumper-selectable pulse-widths to the stimulator, add diode over-voltage protection to the output stage (thus limiting the current), and to replace the exponent adjustment potentiometer with a logarithmic element. We are also likely to return to a modular construction so that well-tested components, such as the power supplies can be constructed using compact, fixed layouts (printed circuit boards) whereas more variable sections such as the analog unit will be constructed to permit adjustment or replacement of key components.

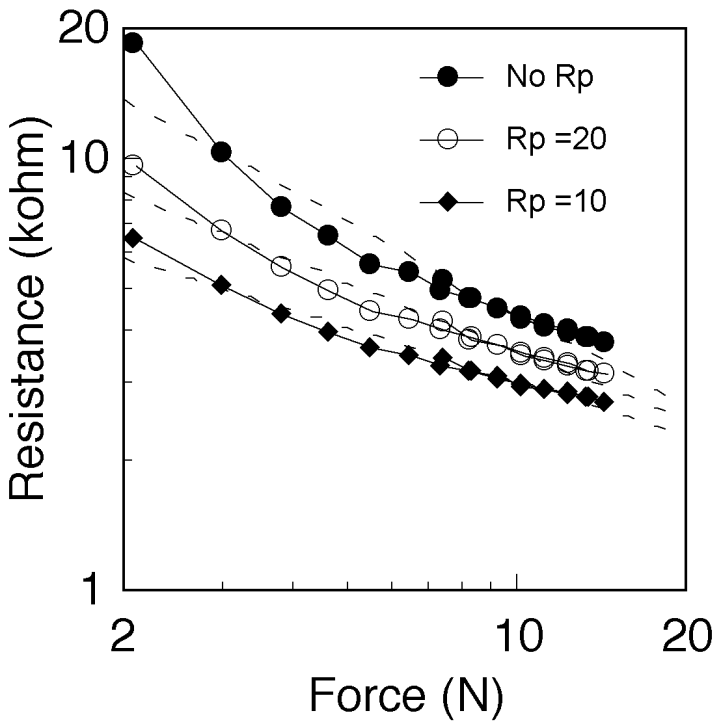

Fig. 2.a.1. Resistance characteristic of an FSR-force sensor with and without “adjustment” resistors (values in kohms) in parallel .

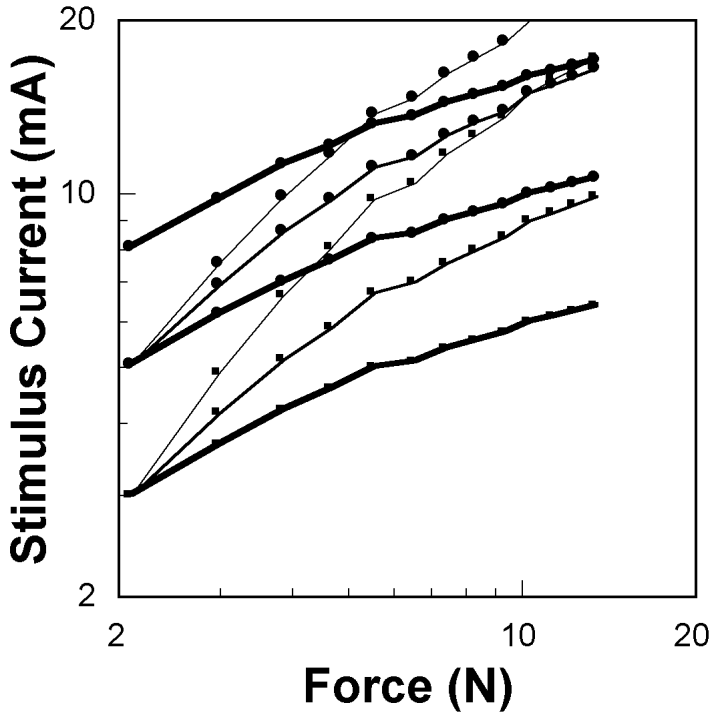

Fig. 2.a.2 Simulated input-output characteristics as a function of threshold and exponent parameters, derived from the resistor characteristic shown above, using a parallel resistance of 5K, and power function exponents >1.

Plans for Next Quarter

Our primary goal will be to complete the revisions described above and construct a third prototype of the grasp-force sensory feedback system.

2. b. INNOVATIVE METHODS OF CONTROL AND SENSORY FEEDBACK

2. b. i. ASSESSMENT OF SENSORY FEEDBACK IN THE PRESENCE OF VISION

Abstract

As planned last quarter, we have started to write a detailed, user-friendly manual for using the video-based neuroprosthesis simulation system.

Purpose

The purpose of this project is to develop a method for including realistic visual information while presenting other feedback information simultaneously, and to assess the impact of feedback on grasp performance. Vision may supply enough sensory information to obviate the need for supplemental

proprioceptive information via electrocutaneous stimulation. Therefore, it is essential to quantify the relative contributions of both sources of information.

2. b. ii. INNOVATIVE METHODS OF COMMAND CONTROL

Abstract

The purpose of this project is to develop new command control algorithms that will make control of neural prosthetic hand grasp simpler and more effective. During this quarter statistical analysis was conducted on the data collected during the last quarter. The data were examined using a generalized linear model that incorporated generalized estimating equations. The coefficients from that model were compared to generate a performance ranking of the algorithms using contrast analyses.

Purpose

The purpose of this project is to improve the function of the upper extremity hand grasp neuroprosthesis by improving user command control. We are specifically interested in designing algorithms that can take advantage of promising developments in (and forthcoming availability of) alternative command signal sources such as EMG, and afferent and cortical recordings. The specific objectives are to identify and evaluate alternative sources of logical command control signals, to develop new hand grasp command control algorithms, to evaluate the performance of new command control sources and algorithms with a computer-based video simulator, and to evaluate neuroprosthesis user performance with the most promising hand grasp controllers and command control sources.

Progress Report

1. Algorithm Names

The names of the algorithms were changed from the names used in the previous reports. The new algorithm names use the descriptive features of the algorithms for identification. The three features tested in addition to proportional control were the rectification feature, the variable-gain feature, and the gated-ramp feature. The new algorithm names are the proportional control algorithm (formerly the baseline algorithm), the rectification algorithm (formerly the proportional rectified-lock algorithm), the rectification gated-ramp algorithm (formerly the threshold rectified-lock algorithm), the rectification variable-gain algorithm (formerly the variable-gain rectified-lock algorithm), and the gated-ramp algorithm (formerly the threshold gated-ramp algorithm). The lock-only algorithm and the variable-gain algorithm retained their names.

2. Data Analysis

The data collected in this study were from a repeated measures design and the response was binary. The data were analyzed using a generalized linear model that incorporated generalized estimating equations for parameter estimation. Factors in this model included the data set, session within each data set, window size, and algorithm.

The equation that describes the linear model using the standard format with the logit link is:

$$E(Y) = Log(\frac{\theta}{1-\theta}) = \beta_0 + \beta_1 X_1 + \beta_2 X_2 + \beta_3 X_3 ...$$

E(Y) is the mean log-odds ratio of the predicted success rate, X_n is a binary variable to indicate the level of a particular factor term, and the β_n values are coefficients of the model that determined how much the level of each factor affected the output of the model. The values of the β_n terms are determined through an iterative process using maximum likelihood estimators. This model was run using SAS software.

Contrast analyses were used to compare the coefficients of the lock-only algorithm to the coefficients of each of the other algorithms (excluding the proportional control algorithm). Since five comparisons were made, a Bonferroni adjusted p-value of 0.01 was used to test for statistical significance.

3. Analysis Results

Figure 2.b.ii.1 contains success rate curves for each algorithm, pooled across data sets and subjects. The success rate varied with each algorithm and window size. The general trend of algorithm performance remained fairly constant between subjects, especially at the middle window size. These results were confirmed by the statistical analysis, which indicated that all window sizes and both data sets were significant effects in the model. The analysis of the window size factor indicated that the

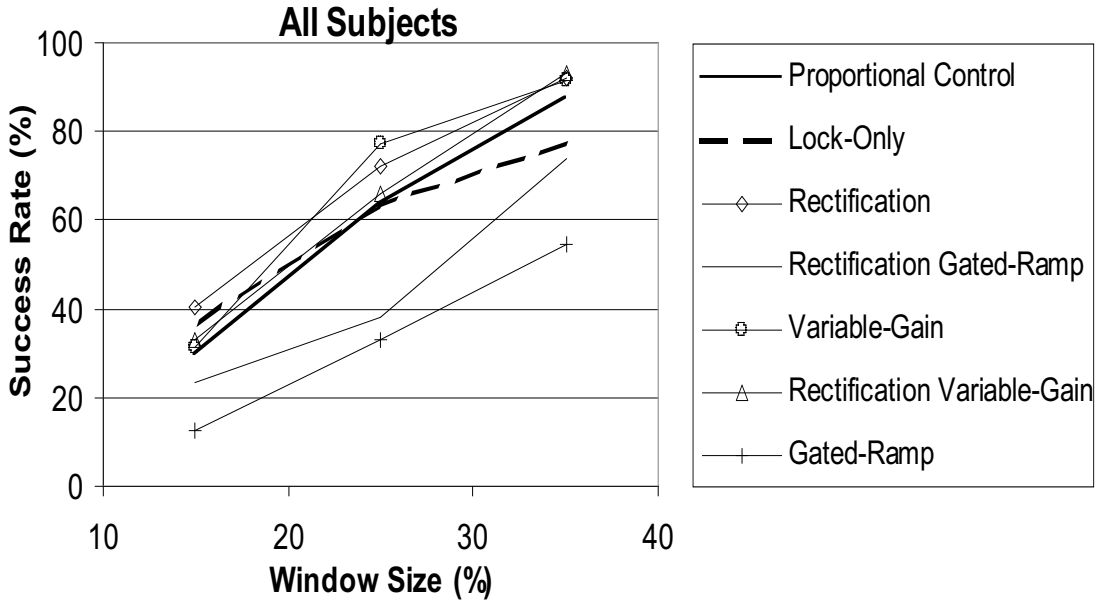

Figure 2.b.ii.1 Success rate on the acquire-hold-modify task as a function of force window size using each of the seven command control algorithms being. Each curve is pooled across data sets and subjects.

success rates increased as the window size increased. The data set model term was significant due to a learning effect across the data sets (higher results were obtained in the second data set). Plots of the

success rate against various combinations of the control variables suggested that most higher order interactions were not important, so these interactions were ignored in the model.

The estimated coefficients for each algorithm are shown in Figure 2.b.ii.2. The error bars represent the 95% confidence interval around the coefficient. The only higher order interaction that was important in this model was between the data set and the session within the set. That interaction does not affect the algorithm term, and thus, the algorithms could be directly compared via contrast analyses.

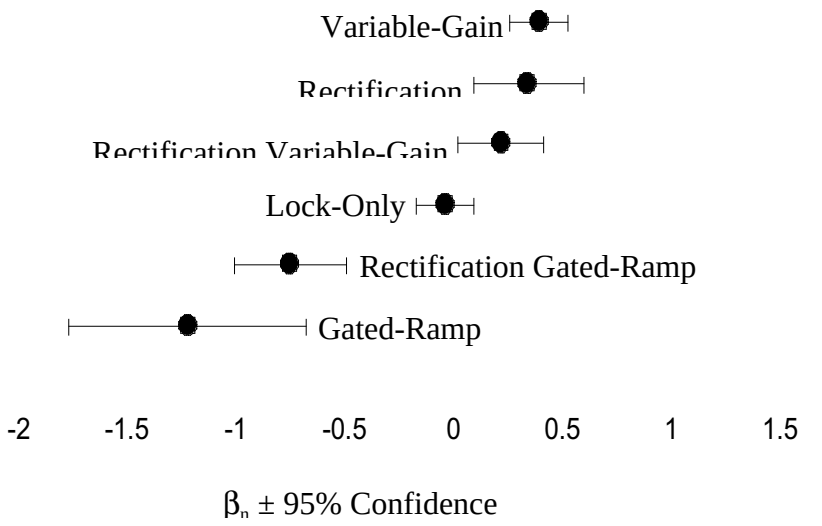

Figure 2.b.ii.2 Graphical comparison of the estimated coefficients for each algorithm in the generalized estimating equations based linear model.

The p-values that resulted from the contrast analyses between the coefficient of the lock-only algorithm and the coefficients of each of the other algorithms are shown in Table 2.b.ii.1.

Algorithm	P-value
Variable-Gain	0.0001
Rectification	0.0094
Rectification Variable-Gain	0.0348
Rectification Gated-Ramp	0.0001
Gated-Ramp	0.0001

Table 2.b.ii.1 Contrast analyses for pair-wise comparisons of the coefficients of each algorithm in the model with respect to the coefficient of the lock-only algorithm. The p-value gives the probability that the effects the two algorithms had on the model were not significantly different. A p-value under 0.01 indicated significance.

As is indicated by the table and graph, the variable-gain and rectification algorithms both yielded significantly higher performances than the lock-only algorithm. Additionally, the rectification variable-gain algorithm, while having a higher mean performance, did not exhibit a statistically better performance than the lock-only algorithm. Finally, the gated-ramp and rectification gated-ramp algorithms yielded significantly lower performances than the lock-only algorithm.

Plans for Next Quarter

In the next quarter, further analysis will take place and the final results will be prepared for publication.

2. b. iii . INCREASING WORKSPACE AND REPERTOIRE WITH BIMANUAL HAND GRASP

Abstract

Further development and assessment of the EEG interface to the hand grasp neuroprosthesis was completed. Working with one neuroprosthesis user, three algorithms to convert the EEG signal into a command input to the hand grasp system were evaluated qualitatively. Of the three, the subject preferred the hold switch algorithm because of its speed and a feeling of better control over hand grasp. The performance of the algorithm was then tested using the Grasp and Release Test (GRT). Results indicate some improvement over time, but overall performance of the existing controllers are still more favorable.

Purpose

The objective of this study is to extend the functional capabilities of the person who has sustained spinal cord injury and has tetraplegia at the C5 and C6 level by providing the ability to grasp and release with both hands. As an important functional complement, we will also provide improved finger extension in one or both hands by implantation and stimulation of the intrinsic finger muscles. Bimanual grasp is expected to provide these individuals with the ability to perform over a greater working volume, to perform more tasks more efficiently than they can with a single neuroprosthesis, and to perform tasks they cannot do at all unimanually.

Progress Report

During the last quarter, effort continued on the development of the EEG interface to the hand grasp neuroprosthesis, specifically on the development of an algorithm to convert the EEG signal into a command input to control hand grasp. In the previous report, we briefly discussed two algorithms that could be used for the transformation of the EEG into a command signal. Both of these algorithms were based upon the fact that subjects have only been able to exhibit a binary level of control over the frontal beta rhythm. The beta rhythm was either present or slightly elevated, or the rhythm was suppressed.

The first algorithm presented was the ‘hold switch’ algorithm. In the operation of this program, a suppression of the frontal beta rhythm below a set threshold initiated a ramp signal to close the hand at a fixed rate until full hand closure was achieved. The command to maintain the hand in a closed posture was only achieved while the EEG signal was below the threshold. When the EEG signal returned to above the threshold value, the command signal was reversed and the hand opened at a fixed rate until full hand opening was achieved. To prevent inadvertent changes to the command signal, a delay of 200 ms, or two sampling periods, was introduced to prevent spontaneous beta rhythm bursts from generating a command signal.

The second algorithm developed was the ‘toggle’ algorithm. Like the hold switch algorithm, it was also based upon the subject’s ability to suppress the frontal beta rhythm below a threshold level. However, instead of only generating a command to close the hand, the suppression of activity generated either a command to open or closed the hand, based upon the current state of the system. Each time the signal went below threshold, the command direction was reversed. If the hand was open and the threshold exceeded, the command was sent to the neuroprosthesis to close the hand; if the hand was closed, by exceeding the threshold the command was sent to open the hand. Also in this algorithm was an introduction of a 200 ms delay to prevent inadvertent activity from generating an unwanted command.

The final algorithm which was developed, and which has not been reported on previously, was a modification of the hold switch algorithm, referred to as the ‘lock’ algorithm. Again, like the other two, the functioning of this algorithm was based upon the subject’s ability to suppress the frontal beta activity. The hand started initially in the closed position, whereas the other two algorithms started with the hand open. Upon the suppression of the beta activity below the threshold level, the hand was opened at a fixed rate until full hand opening was achieved. When the signal went back above the threshold, the command was sent to closed the hand and maintain it in a closed position. This was an attempt to instill a locking mechanism into the EEG controller so that the subject could relax once an object was achieved and not worry about losing their grasp. This algorithm was also modified as follows: 1) the delay was removed to allow for a faster response of the system, 2) and the threshold was set at a much higher level since it was observed that the spontaneous bursts of EEG activity did not return the signal to the previous resting baseline resting level.

One neuroprosthesis user tested all three algorithms. This is the same individual who has been reported on previously. He was selected for the development of the algorithms because of his experience with frontal beta control and with using the EEG interface. Each of the algorithms was tested during three separate sessions, each lasting two to three hours. The subject was first instructed on how the algorithm would operate, and then given as much time as he felt necessary to learn to control his hand grasp using the algorithm. The subject was given the objects of the Grasp and Release Test (GRT) to practice with, and tested the algorithms using both the lateral and palmar grasp. While the subject was

practicing, the rate at which he could open and close his hand was recorded. He was also asked to report his thoughts and insights into the operation of the algorithms.

Of the three algorithms developed, the one which performed the best and which the user preferred was the hold switch algorithm. The toggle algorithm, because of the delays introduced and the fact that the subject had to return to the resting level before he could change command directions was unacceptably slow to the user. The time to open and close the hand was recorded as requiring 6.0 (+/-1.3 S.D.) seconds on average. Also, a great deal of confusion was encountered in keeping track of whether the hand was just recently opened or closed, as thus what command would be issued to the system upon suppression of the beta activity. The lock algorithm, although faster than the lock switch algorithm (2.1 +/- 0.8 compared to 3.0 +/- 1.5 seconds) and providing a means to secure grasp upon an object, was also unacceptable to the user because he felt that he did not have full control over the neuroprosthesis. Because of the higher threshold level, when the subject was resting the hand tended to open and close slightly as the resting state of the EEG signal slowly oscillated above and below the threshold value.

The testing of the three algorithms with the neuroprosthesis user led to the conclusion that only the hold switch algorithm would be tested will future neuroprosthesis users. However, there was still a need to allow for the user to lock the hand into place once an object was secured in the grasp. Therefore, the EEG interface was modified to allow for the incorporation on an external push-button switch. The switch in this case performs the same function as the external switch found as part of the shoulder controller provided with the Freehand system. By pressing the switch once, the neuroprosthesis is turned on. From that point on, any time the subject presses the switch again, a command will be issued to lock and unlock the system. By pressing and holding the switch, the subject can then shut the neuroprosthesis off. The introduction of this external switch allows the neuroprosthesis user to have the same functionality with the EEG controller as they would have with any of the existing controllers. The only difference is that the subject is still unable to change hand grasps with the EEG controller. The inability to change hand grasps, however, cannot be addressed for as long as a computer interface is needed to provide a command input to the ECU.

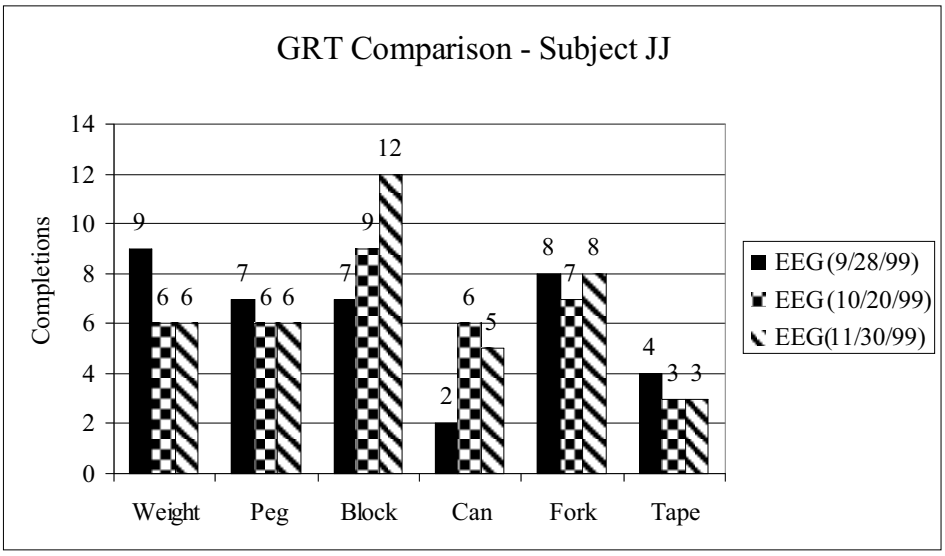

Figure 2.b.iii.1 - GRT Comparison for the EEG interface

The definition of the control algorithm and the introduction of the external switch then allowed for further testing of the EEG interface. To achieve this, the subject was tested three times with the controller on the grasp and release test. These testes were spaced approximately one month apart, and during the intervening time, the subject practiced using the EEG controller in the lab. The results of the GRT tests for each of the six objects is shown in Figure 2.b.iii.1. The values given are of the median number of completions during the three trials of the GRT. From this figure, it can be seen that subject performance remained fairly constant over time, except for the block that improved slightly with training. Also, the number of completions (with the exception of the blocks) also remained consistent across objects, with no improvement over time.

The results from these tests provide further indication that there are certain inherent delays in the system which limit how quickly the interface can be used. This was first described in the previous progress report, were the results of the GRT with the EEG interface showed the same consistent performance across objects, and is further verified by the fact that additional training on the operation of the interface does little to improve performance. To determine where the delays are occurring, an additional experiment was performed with the subject. Modifying the EEG interface, the computer was set up to record the EEG voltages derived from the FFT analysis on the beta band, as well as to record the press of an external switch. Then, running the interface, the subject was given the verbal command to close his hand (which was then recorded with a press of the switch), and the change in the EEG signal and command level to the neuroprosthesis was recorded every 100 ms as the subject fully closed his hand. This was then repeated 20 times, and the times for the EEG signal to drop 10%, to exceed the threshold value, and for the command level to change were recorded.

The results of this experiment indicated that, in addition to the 200 ms delay which was inherent in the command algorithm, there was an additional 300 (+/- 250 ms S.D.) delay between the time the command was given to close the hand and the time when the EEG signal responded with a 10% drop in

the FFT voltage. These results compare favorably with the studies by Tallon-Baudry [1], Basar [2] and Fernandez [3], who have studied the frontal beta and gamma rhythms during cognitive processing in humans. They found a change in either the beta or gamma rhythms in the frontal areas, occurring 300 ms after the subject began on the computation of a cognitive intensive task (i.e. visual search task or numerical operations). They therefore considered the frontal rhythm changes to be similar to an visual or motor evoked potential in the latency of response, although this was in response to cognitive changes and not changes in external stimuli. The results from our study would tend to support this finding, as well as help support our claim that the signal we are recording from is indeed a cortical signal and not an EMG response.

Plans for Next Quarter

During the next quarter, testing will be completed on the EEG interface with the one neuroprosthesis user using the Activities of Daily Living (ADL) assessment. It is believed that the performance of the EEG controller will be comparable to the existing controllers on a test that is based on performance instead of time. Also, two additional neuroprosthesis users will be trained on using the EEG interface, and then tested using the GRT to assess whether other individuals can use the EEG controller for their hand grasp system.

References

C. Tallon Baudry, O. Bertrand, C. Delpuech, and J. Pernier. " Oscillatory gamma-band (30-70 Hz) activity induced by a visual search task in humans", Journal of Neuroscience, vol. 17(2), pp. 722-734, 1997.

E. Basar, C, Basar-Eroglu, S. Karakas, and M. Schumann. "Are cognitive processes manifested in event-related gamma, alpha, theta and delta oscillations in EEG?", Neuroscience Letters, vol. 259, pp. 165-168, 1999.

T. Fernandez, T. Harmony, M. Rodriquez, J. Bernal, J. Silva, A. Reyes, and E. Marosi. "EEG activation patterns during the performance of tasks involving different components of mental calculation", Electroencephalography and Clinical Neurophysiology, vol. 94, pp. 175-182, 1995.

2. b. iv CONTROL OF HAND AND WRIST

Abstract

The structure for software for training and testing the performance of a feedforward control system for hand grasp and wrist performance has been completed. The combined hardware/software system has been constructed using commercially available high-level software, simplifying implementation, modification, and maintenance.

Purpose

The goal of this project is to design control systems to restore independent voluntary control of wrist position and grasp force in C5 and weak C6 tetraplegic individuals. The proposed method of wrist command control is a model of how control might be achieved at other joints in the upper extremity as well. A weak but voluntarily controlled muscle (a wrist extensor in this case) will provide a command signal to control a stimulated paralyzed synergist, thus effectively amplifying the joint torque generated by the voluntarily controlled muscle. We will design control systems to compensate for interactions between wrist and hand control. These are important control issues for restoring proximal function, where there are interactions between stimulated and voluntarily controlled muscles, and multiple joints must be controlled with multijoint muscles.

Progress Report

In the previous quarter, we looked at the performance and compatibility characteristics of Windows NT and selected it as the platform for the computer system, which consists of 2 phases: training and real-time control. The training phase is used to collect and analyze data to be used in the real-time control of grasp output and wrist postion.

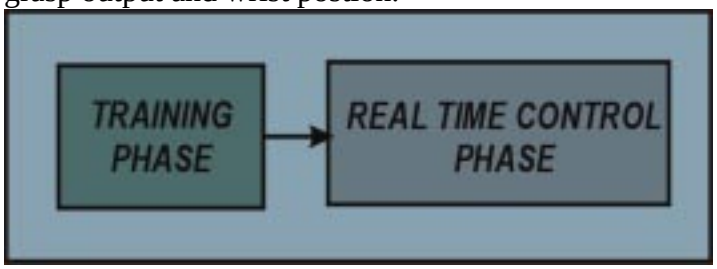

Figure 2.b.iv.1 Two part structure of the feedforward hand grasp/wrist control software.

The training phase consists of many different trials, in which the muscles are stimulated at different levels and the muscle responses are measured and stored for analysis. The training phase also includes the analysis of muscle responses to obtain a data set to train the neural network, and the actual training of the network(s).

The real-time control phase includes measurement of the command and feedforward inputs, the feedforward estimation of stimulation parameters, and the control of stimulation. Since this is an experimental system, the real-time control phase also includes the option of computer generated command signals and measurement of various sensors to measure the system output. These are required to characterize the quality of control.

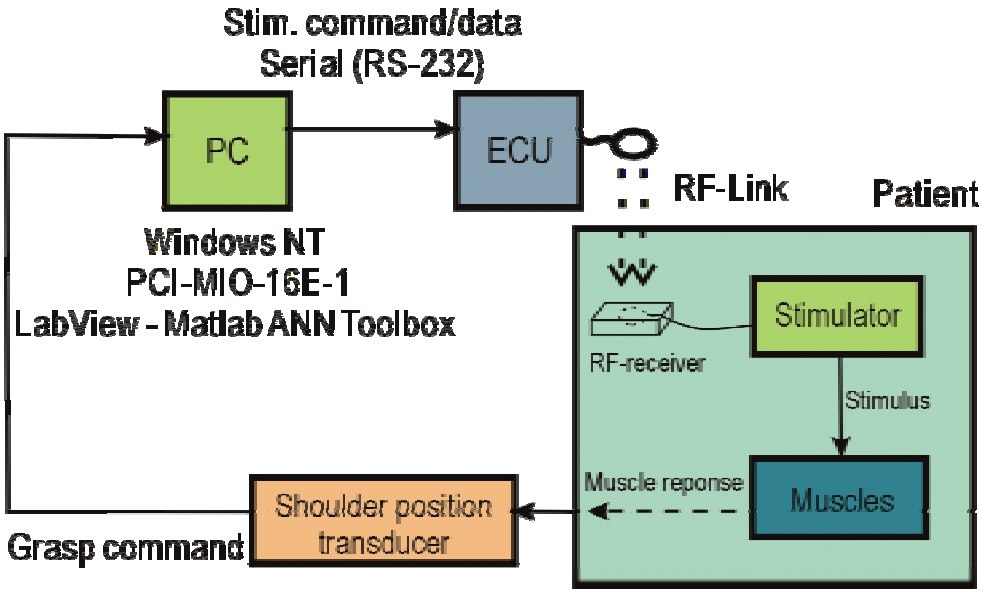

Figure 2.b.iv.2 Block diagram of the hand grasp/wrist control system.

The computer system has been implemented using Matlab Neural Networks Toolbox© to create the neural network, and LabView© to develop the rest of the software. This control program also uses the PCI-MIO National Instruments data acquisition board installed on the PC.

The flowchart organization of the software is shown in Figure 2.b.iv.3. There are parallels between the training and real-time control phases, since both involve real-time control of stimulation and data collection. The difference is that stimulation parameters are obtained from files of stimulus parameters to collect the training data, whereas in the real-time control phase, the stimulus parameters are obtained from a real-time operation of the trained neural network. The ability of the system to perform the real-time calculations was demonstrated in the previous quarterly progress report.

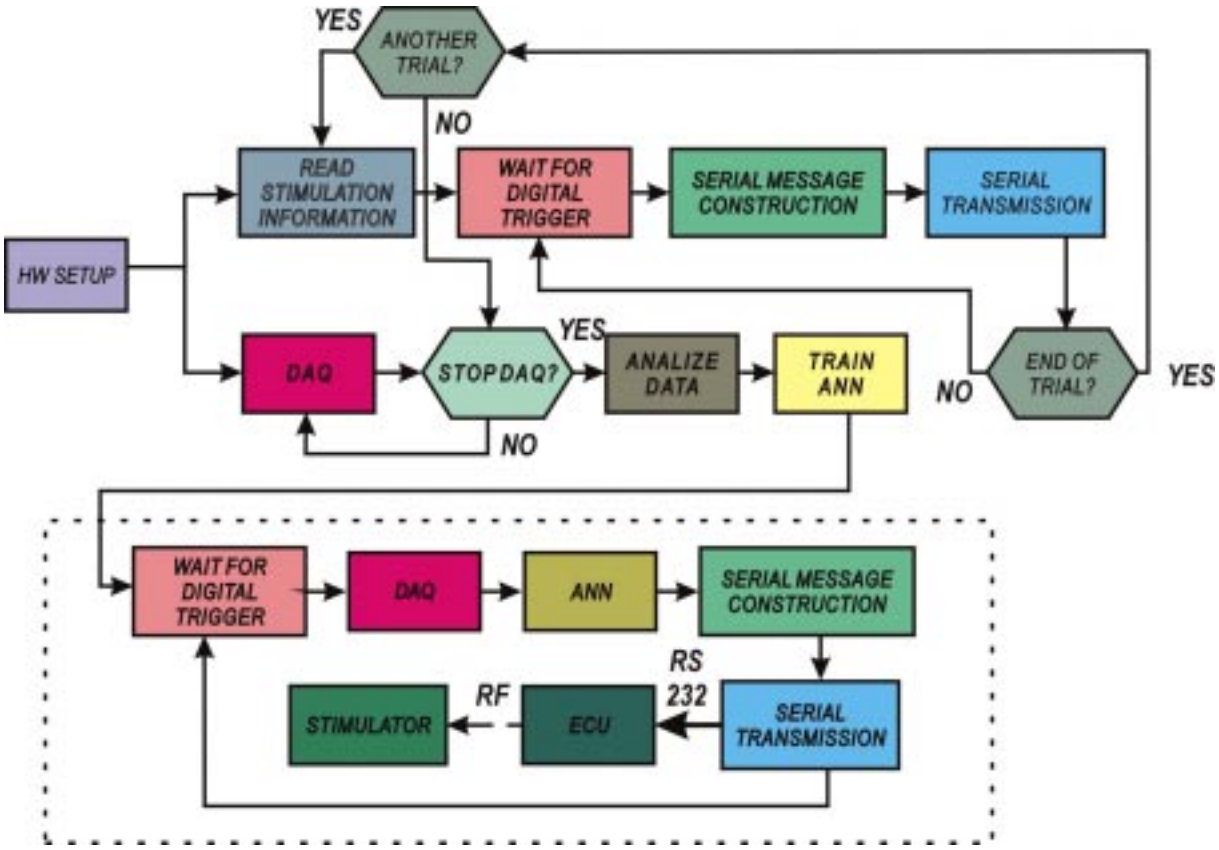

Figure 2.b.iv.3. Flowchart organization of the training (top) and real-time control (bottom, in dotted box) phases of the software.

Although the details of the software will not be described, a few of the user interfaces are shown in Figure 2.b.iv.4. The top interface is the main menu allowing operation of the various parts of the program, while the bottom interface is for the real-time control phase.

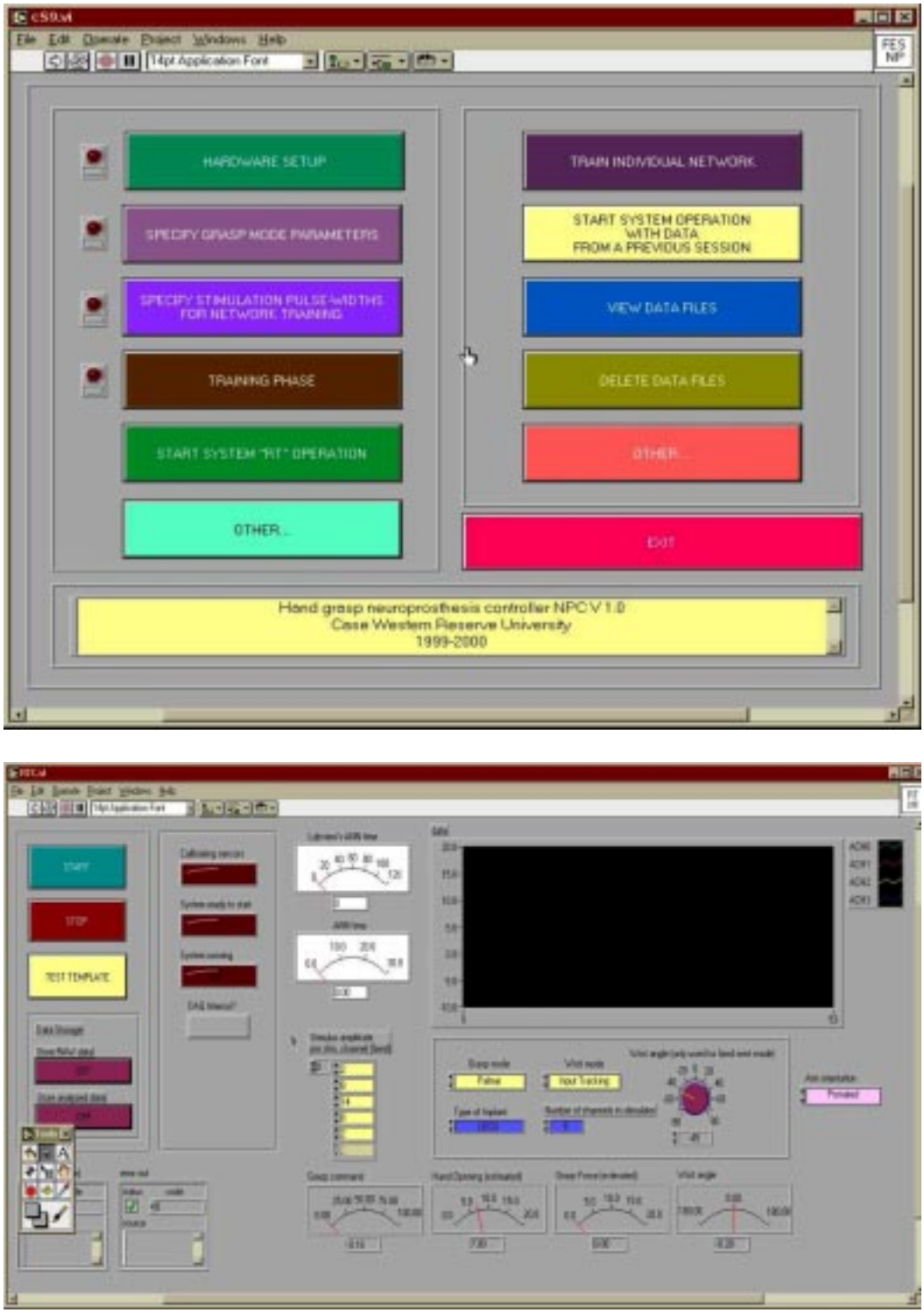

Figure 2.b.iv.4 Two of the user interfaces for the handgrasp/wrist control system software. Top: main control panel. Bottom: real-time control panel.

Plans for next quarter

We will continue to develop and verify the correct operation of the software. No experiments will be scheduled until this has been completed. We expect to begin experiments toward the end of next quarter.